Original Study

Assessment of a Radiomic Signature Developed in a General NSCLC Cohort for Predicting Overall Survival of ALK-Positive Patients With Different Treatment Types

Lyu Huang, Jiayan Chen, Weigang Hu, Xinyan Xu, Di Liu, Junmiao Wen, Jiayu Lu, Jianzhao Cao, Junhua Zhang, Yu Gu, Jiazhou Wang, Min Fan

Abstract

Anaplastic lymphoma kinase (ALK)-positive (ALK$^+$) patients exhibit unique clinical characteristics. It would be beneficial to effectively predict their treatment outcome. We assessed the performance of the radiomic signature from non–small-cell lung cancer for predicting ALK$^+$ patient outcomes using the least absolute shrinkage and selection operator Cox regression model. Its performance was impaired when used for ALK$^+$ patients treated with tyrosine kinase inhibitors (TKIs). Therefore, developing special signatures for patients treated with TKIs might be needed.

Background: The purpose of the study was to investigate the potential of a radiomic signature developed in a general non–small-cell lung cancer (NSCLC) cohort for predicting the overall survival of anaplastic lymphoma kinase (ALK)-positive (ALK$^+$) patients with different treatment types. **Materials and Methods:** After test-retest in the Reference Image Database to Evaluate Therapy Response data set, 132 features (intraclass correlation coefficient > 0.9) were selected in the least absolute shrinkage and selection operator Cox regression model with a leave-one-out cross-validation. The NSCLC radiomics collection from The Cancer Imaging Archive was randomly divided into a training set ($n = 254$) and a validation set ($n = 63$) to develop a general radiomic signature for NSCLC. In our ALK$^+$ set, 35 patients received targeted therapy and 19 patients received nontargeted therapy. The developed signature was tested later in this ALK$^+$ set. Performance of the signature was evaluated with the concordance index (C-index) and stratification analysis. **Results:** The general signature had good performance (C-index > 0.6; log rank $P < .05$) in the NSCLC radiomics collection. It includes 5 features: Geom_va_ratio, W_GLCM_Std, W_GLCM_DV, W_GLCM_IM2, and W_his_mean. Its accuracy of predicting overall survival in the ALK$^+$ set achieved 0.649 (95% confidence interval [CI], 0.640-0.658). Nonetheless, impaired performance was observed in the targeted therapy group (C-index = 0.573; 95% CI, 0.556-0.589) whereas significantly improved performance was observed in the nontargeted therapy group (C-index = 0.832; 95% CI, 0.832-0.852). Stratification analysis also showed that the general signature could only identify high- and low-risk patients in the nontargeted therapy group (log rank $P = .00028$). **Conclusion:** This preliminary study suggests that the applicability of a general signature to ALK$^+$ patients is limited. The general radiomic signature seems to be only applicable to ALK$^+$ patients who had received nontargeted therapy, which indicates that developing special radiomics signatures for patients treated with tyrosine kinase inhibitors might be necessary.

Clinical Lung Cancer, Vol. 20, No. 6, e638-51 © 2019 Published by Elsevier Inc.

Keywords: ALK rearrangement, Carcinoma, Non–small-cell lung, Multislice computed tomography, Survival analysis

L.H. and J.C. contributed equally to this work as first authors.

Department of Radiation Oncology, Fudan University Shanghai Cancer Center, Shanghai, China

Submitted: Feb 6, 2019; Revised: Apr 8, 2019; Accepted: May 3, 2019; Epub: May 11, 2019

Addresses for correspondence: Min Fan, PhD, MD or Jiazhou Wang, PhD, Department of Radiation Oncology, Fudan University Shanghai Cancer Center, No 130 Dong'An Road, Xuhui district, Shanghai 200032
E-mail contact: wjiazhou@gmail.com; fanming@fudan.edu.cn

1525-7304/$ - see frontmatter © 2019 Published by Elsevier Inc.
https://doi.org/10.1016/j.cllc.2019.05.005

Introduction

In the past few years, anaplastic lymphoma kinase (ALK) rearrangements, either inversions or translocations, were identified as driver mutations in non–small-cell lung cancer (NSCLC).[1,2] An echinoderm microtubule-associated protein like 4 (EML4)-ALK fusion is the most common mutation and was first identified by Soda et al in 2007.[3] The EML4-ALK fusion mainly occurs in young people, never-smokers, and light smokers with lung adenocarcinoma.[4] Patients with ALK rearrangements usually exhibit unique clinical characteristics. Oncologists need effective tools to predict and improve their treatment outcome.[5]

Radiomics is an emerging field that extracts advanced features from noninvasive images using automatic algorithms to quantitatively characterize tumors. Radiomics assumes the underlying association between multimodality images and pathophysiology.[6-9] Various prognostic or predictive radiomic signatures have been developed and well validated in NSCLC patients.[10-17] These studies suggest that radiomics could reveal tumor characteristics and thus be a useful tool for oncologists.[18]

Signatures that are on the basis of common attributes of NSCLC patients are called general radiomic signatures. It is unknown whether a general radiomic signature could perform well in patients with genetic mutations, because unlike typical patients, those with a driver mutation have distinct clinical characteristics.[19] Studies have shown that a single radiomics signature can be applied to different cancers.[14,20] Aerts et al[14] reported that a radiomic signature has a fair performance in lung cancer patients (concordance index [C-index] = 0.65) and head-and-neck cancer patients (H&N1: C-index = 0.69; H&N2: C-index = 0.69). This result indicates that a radiomic signature might be useful to general and unique (eg, ALK-positive [ALK^+] patients).

Crizotinib is a selective inhibitor of ALK, and Shaw et al[21] showed that crizotinib is superior to standard chemotherapy for advanced stage patients with an ALK rearrangement. It is unknown whether tyrosine kinase inhibitors (TKIs) would affect the accuracy of a general radiomic signature if patients received targeted therapy.

The purpose of this study was to investigate the performance of a general radiomic signature in ALK^+ patients. First, we developed a signature from NSCLC patients. Then, we investigated whether our general radiomic signature could predict the overall survival (OS) of patients with the ALK rearrangement. Last, we investigated the effect of treatment types on the signature's performance.

Materials and Methods

The main work flow is presented in Figure 1. First, we used the Reference Image Database to Evaluate Therapy Response (RIDER) data set to obtain stable features. Then, we used those features to develop a general radiomics signature. This radiomics signature was tested in our ALK^+ patient cohort.

Patients

Ethical approval was obtained for this retrospective analysis, and the requirement for informed consent was waived. Data from 2 cohorts of clinical patients from Dutch and Chinese cancer centers were included. Dutch patients (n = 317) in the NSCLC radiomics collection received radiotherapy or chemoradiotherapy at the Maastro Clinic.[14,22,23] Their genetic profiles were not disclosed. Their images, segmentation, and clinical data were downloaded directly from The Cancer Imaging Archive Web site.

Figure 1 Analysis Work Flow. The Radiomic Features Extraction Code Set Was Applied to 3 Different Data Sets

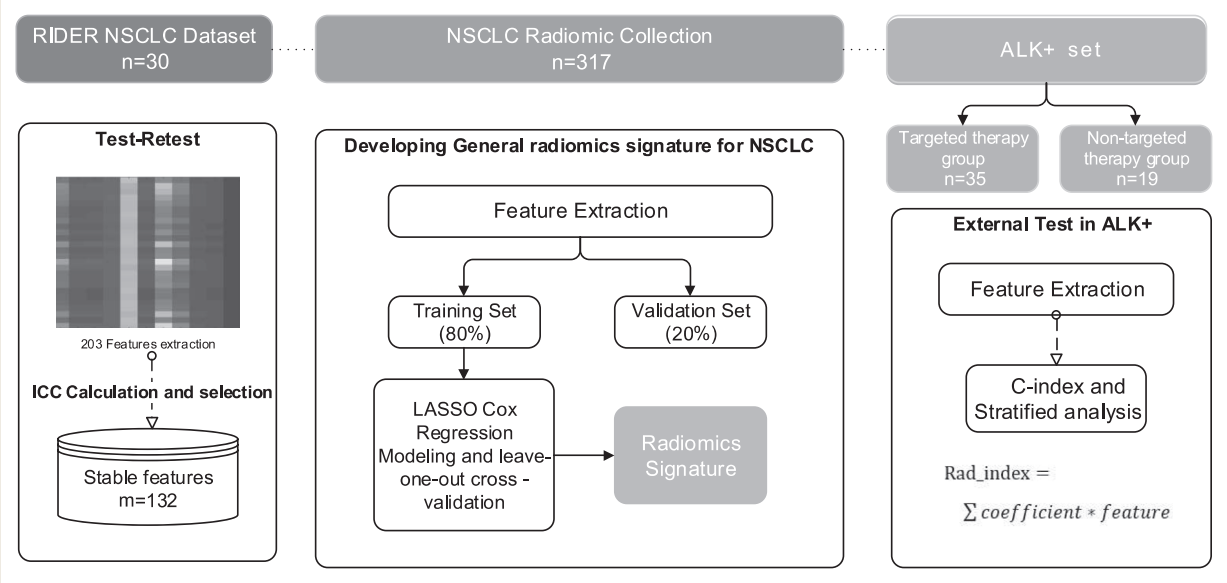

Abbreviations: ALK = anaplastic lymphoma kinase; ICC = intraclass correlation coefficient; LASSO = least absolute shrinkage and selection operator; m = number of stable features; n = patient number; NSCLC = non–small-cell lung cancer; RIDER = The Reference Image Database to Evaluate Therapy Response.

Patients treated at Fudan University Shanghai Cancer Center (FUSCC) from June 2014 to December 2016 were reviewed. The eligibility criteria were as follows: (1) patients were histologically confirmed to have NSCLC, and their records could be retrieved through the electronic medical record system; (2) patients received only chemotherapy, radiochemotherapy, or targeted therapy; (3) the pretreatment computed tomography (CT) and radiotherapy structure using the Pinnacle treatment planning system (8.0 m; Philips Healthcare, Andover, MA) and MIM (version 6.6, MIM Software Inc, Cleveland, OH) were available; and (4) ALK rearrangement was confirmed in tumor samples using immunohistochemistry and fluorescent in situ hybridization analysis.

A total of 54 patients met all of the inclusion criteria. Patients in the ALK^+ set were divided into a targeted therapy group (n = 35) and a nontargeted therapy group (eg, chemotherapy or chemoradiotherapy; n = 19). Tumor staging was on the basis of the American Joint Committee on Cancer Tumor, Node, Metastases Staging Manual, 7th edition.

Follow-up

The end point of this study was OS, which was defined as the time from the day of diagnosis until either the day of death (event) or until the date that the patient was last known to be alive (censored).[24]

Computed Tomography Acquisition and Segmentation

In the ALK^+ set, pretreatment CT was obtained with a Sensation 64 or a Biograph 16 positron emission tomography/CT scanner (Siemens Healthineers) using a standard clinical scanning protocol. Thoracic CT scans were acquired without intravenous contrast, and images were reconstructed using the reconstruction kernels of B31f or B30f. The primary tumor was delineated manually using MIM software by an experienced oncologist. Boundaries with chest and other soft tissues were identified first at the abdominal window (width [W]: 400; length [L]: 50), then we changed to the lung window (W: 1700; L: −300) for contouring. All of the delineations were reviewed by another oncologist. The contours in the NSCLC Radiomic Collection were also checked.

Features Extraction and Test-Retest Reliability

An in-house feature extraction code set on the basis of MATLAB (version 2015b; Mathworks, Natick, MA) was used (see Supplemental Appendix A: Radiomic Features Extraction). Our in-house radiomics codes could extract 873 features. Because of the size of our training set (approximately 300), we only used the absolute type in histogram features and average type in textural features. In total, 203 features were extracted from CT scans, and these features were classified into 7 groups: (1) geometry features; (2) histogram features; (3) gray level co-occurrence matrix-based features; (4) gray level run-length matrix-based features[25]; (5) wavelet gray level cooccurrence matrix-based features; (6) wavelet gray level run-length matrix-based features; and (7) wavelet histogram-based features (see Supplemental Table 1 in the online version).

The RIDER test-retest data set[26-28] was used to find the most stable features between 2 interval CT scans. In total 31 patients were included. The primary tumor was segmented in test scans and retest scans using the Grow Cut algorithm in 3D Slicer (version 4.7.0).[29,30] The segmentation results were examined by an experienced oncologist. Both scans of a single patient were extracted for radiomics features according to in-house codes. Stability was assessed using the intraclass correlation coefficient (ICC). In this study, a 2-way fixed effect, absolute agreement, and single measurement model was selected for ICC calculation.[31] The ICC was defined as follows:

$$\mathrm{ICC} = \frac{MS_R - MS_E}{MS_R + (k-1)MS_E + \frac{k}{n}(MS_C - MS_E)} \quad \text{Equation 1}$$

where MS_R indicates the mean square for rows; MS_E the mean square for error; MS_C the mean square for columns; n the number of patients; and k the number of scans. Features with ICC >0.9 were considered stable.

Statistical Analysis

Statistical analysis was performed using R software (version 3.3.2; http://www.R-project.org). The reported significance levels were all 2-sided, and the statistical significance level was set at 0.05.

Construction of General Radiomics Signature. The NSCLC Radiomic Collection was divided into training (80%) and validation (20%) partition using the createDataPartition function in R studio. We used the least absolute shrinkage and selection operator (LASSO) Cox regression analysis with a leave-one-out cross-validation to develop our radiomic signature. The LASSO is a shrinkage and selection method that implements a penalty function to reduce variable dimension and restrict model size. After the general radiomics signature was developed solely in the training set, we calculated the corresponding radiomic index (Rad_index) for every patient via a linear combination of features multiplied by their coefficients.

Assessment of Prognostic Value of General Signature in ALK^+ Patients.. The general radiomics signature was first assessed in the NSCLC Radiomic Collection, and then tested in the ALK^+ set. The prognostic performance was quantified by using the C-index. The C-index ranges from 0.5 to 1. The higher the C-index, the better the signature. Stratification analysis was also used to evaluate the association with OS. Patients were classified into high-risk or low-risk groups according to Rad_index. The optimal threshold was determined by using the median value of Rad_index in the training set. The log rank test was conducted to evaluate the difference in survival curves between the high-risk and low-risk groups.

Results

Clinical Characteristics

Detailed patient characteristics are shown in Table 1.

In the training set, the median survival was 18.1 months (0.95 confidence limit [CL], 16.0-23.4 months). Most of the patients in the training set were male (71.3%). The median age at the beginning of treatment was 69.9 years of age (range, 42.5-91.7 years). In the validation set, the median survival was 18.2 months (0.95 CL, 14.4-30.2 months). Most of the patients were also male in the validation set (63%), and the median age was 68.3 years of age (range, 46.5-87.1 years).

Table 1 Patient Characteristics and Outcome are Presented for Each Data Set

Characteristic	NSCLC Radiomics Collection		ALK$^+$ Set	
	Training Set (n = 254)	Validation Set (n = 63)	Nontargeted Therapy Group (n = 19)	Targeted Therapy Group (n = 35)
Median Age (Range), Y	69.9 (42.5-91.7)	68.3 (46.5-87.1)	53 (24-77)	53 (33-77)
Sex				
Female	73 (28.7%)	17 (27%)	8 (42.1%)	16 (45.7%)
Male	181 (71.3%)	46 (63%)	11 (57.9%)	19 (54.3%)
Overall Stage				
I	64	17	0	0
II	20	6	1	0
III	169	40	8	8
IV	0	0	10	27
Histology				
Adenocarcinoma	25	6	19	34
Squamous-cell carcinoma	76	15	0	1
NOS	43	13	0	0
Large-cell carcinoma	83	18	0	0
Overall Survival				
Median (0.95 CL)	18.1 (16.0-23.4)	18.2 (14.4-30.2)	20.1 (NA)*	NA*

Abbreviations: ALK = anaplastic lymphoma kinase; CL = confidence limit; NOS = not otherwise specified; NSCLC = non–small-cell lung cancer.
*The median survival or the 0.95 CL is unreachable.

In the ALK$^+$ set, the median age was 53 years in both of the subgroups. Using the Kaplan–Meier estimate of potential follow-up, the median follow-up period was 22.9 months (0.95 CL, 16.9-26 months).

Test-Retest Reliability

On the basis of the RIDER data set, we discovered 132 features of high reliability (ICC > 0.9) and 4 features of poor reliability (ICC < 0.5). Approximately 65% of the tested features had a high reliability, 19% a good reliability (ICC = 0.9-0.75), 14% a moderate reliability (ICC = 0.75-0.5), and 2% a poor reliability. Detailed results are shown in Supplemental Figure 1 and Supplemental Table 2 in the online version.

Construction of General Radiomics Signature

The 132 stable features were put into the LASSO Cox regression model. When the lambda was set at 0.167, we obtained the most simplified model. Five features with nonzero coefficients comprised the general radiomics signature. They were: (1) W_His_mean; (2) W_GLCM_IM; (3) W_GLCM_DV; (4) W_GLCM_Std; and (5) Geom_va_ratio. The coefficient of each feature is presented in Figure 2. The expansions are provided in Supplemental Table 3 in the online version.

The Rad_index was defined as the following formula:

Rad_index = 0.01634 × W_his_mean − 0.01389 × W_GLCM_IM − 0.02765 × W_GLCM_DV − 0.02723 × W_GLCM_Std + 0.03799 × Geom_va_ratio.

The median value of Rad_index in the training set was 0.02056. Accordingly, patients were classified into a high-risk (Rad_index ≥ 0.02056) or low-risk (Rad_index < 0.02056) group.

Assessment of the Prognostic Value of the General Signature in ALK$^+$ Patients

The 5-feature signature had good performance in the training set (C-index = 0.632; 95% confidence interval [CI], 0.630-0.634) and the validation set (C-index = 0.621; 95% CI, 0.616-0.626). We also observed a C-index of 0.649 (95% CI, 0.640-0.658) in the ALK$^+$ set. The nontargeted therapy group exhibited a higher C-index (0.842; 95% CI, 0.832-0.852) than the targeted therapy group (0.573; 95% CI, 0.589-0.556).

In the stratification analysis, the performance (log rank $P = .038$) in the validation set showed that the Rad_index could identify high-risk or low-risk patients with NSCLC. However, in the ALK$^+$ set, only patients treated with nontargeted therapy could be accurately classified into the correct groups (log rank $P = .0028$). the Kaplan–Meier curves of high-risk and low-risk groups from all of the data sets are shown in Figure 3. Calibration curve is presented in Supplemental Figure 2 in the online version.

Discussion

In this study, we analyzed 203 radiomic features and developed a general radiomics signature for NSCLC patients. This signature is composed of 5 features. W_His_mean calculates the average of grayscale value after wavelet transformation, which represents the overall characteristics of the tumor. W_GLCM_IM, W_GLCM_DV, and W_GLCM_Std are texture features that represent the intratumor heterogeneity. Geom_va_ratio calculates the ratio of volume to surface area and represents the tumor compactness. The selected features are similar to those in other proposed signatures for NSCLC.[13,32-35] Features relating to

Figure 2 Five Features Selected From LASSO Cox Regression Analysis Are Presented. The Coefficient Indicates the Feature's Contribution to the Developed Cox Regression Model (Plotted on the X-Axis)

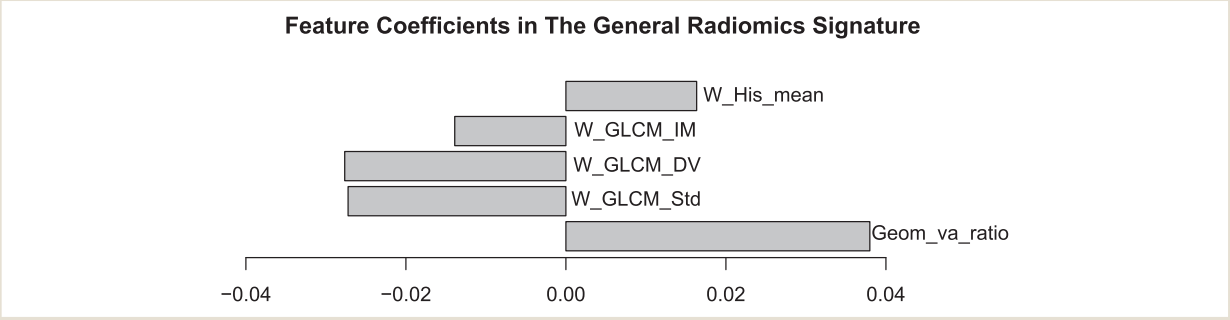

compactness and intratumor heterogeneity were shown to have a strong association with prognosis in NSCLC.

Previous studies on ALK$^+$ tumors have focused on the association between radiomic features and driver gene status.[17,36,37] This work investigated the prognosis of patients with the ALK rearrangements, which is distinctive in methodology.

We found that the general radiomic signature is applicable to ALK$^+$ patients under certain conditions. This signature could predict prognosis of patients treated with nontargeted therapy. However, it cannot make a good prediction for those treated with TKIs. As previously shown, conventional therapy damages all rapidly dividing cells, whereas targeted therapy selectively destroys cancer cells by interacting with a specific molecule and cutting off metabolic pathways in the tumor. A general radiomic signature was usually developed from the common attributes of NSCLC patients who received conventional therapy. Notably, targeted therapy has a different mechanism of action, which could result in a distinctive outcome in ALK$^+$ patients.[21] This difference could be the reason for general signature failure. Our study showed that for patients treated with TKIs, it could be necessary to develop a special

Figure 3 The Stratification Analysis Results in All Data Sets. We Used the Median of Rad_index in the Training Set as a Cutoff Point. Significant Results Are Observed in the Validation Set (P = .035) and the Nontargeted Therapy Group (P = .0028)

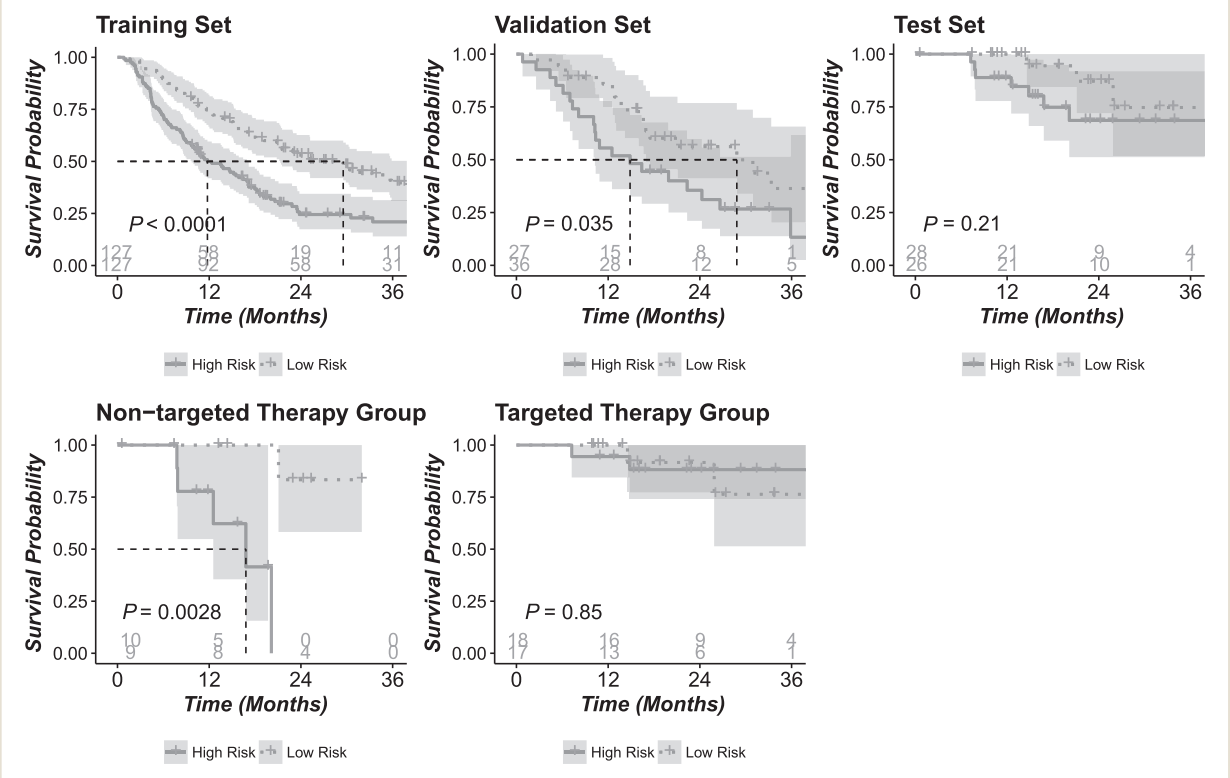

radiomic signature. These radiomic signatures might differ depending on the specific targeted therapy.

In addition, the Kaplan–Meier curves in the targeted therapy group showed that the outcome of predicted high-risk patients was improved by targeted therapy. It further justified the standard form of treatment and proved that targeted therapy is effective for prolonging patients' lives.

Radiomics tools might help to tailor medical treatment to meet individual needs and facilitate the advent of an era of personalized therapy. They have shown their prognostic value in many studies.[12-14,38,39] This study is significant because it points out that general radiomic signatures have limitations when applied to patients who received different types of treatment. The general idea of improving signature performance is to expand the data set and collect more patients. For general patients treated with conventional therapy, this method could make radiomic signature more representative and improve performance. However, our study indicates that the general radiomic signature might still have poor performance in patients treated with targeted therapy because of the different mechanisms between targeted therapy and conventional therapy. Thus, developing a special radiomics signature for a specific group of patients treated with targeted therapy might be another viable method. To that end, oncologists could benefit most from radiomics when this special signature is combined with the general signature for use.

Because of the low incidence of ALK rearrangements in NSCLC, only 54 patients were included in our ALK^+ set. The small data set size is one of the limitations of our study. Meanwhile, we only investigated patients with ALK rearrangements. There are other driver genes, such as epidermal growth factor receptor (EGFR) mutations. As we know, targeted therapy has different mechanisms in killing tumors compared with conventional therapy. Even within patients with gene mutations, the specific targets could be different. This preliminary study cannot answer the question as to whether there is an independent signature for all patients who had received targeted therapy. It is possible that patients with ALK or EGFR mutation need different signatures, because their specific targets and subsequent mechanism might be different. More data are needed to reveal how targeted therapy affects the performance of a general radiomic signature, which is the focus of our ongoing work. We believe that the implementation of radiomic analysis on these patients would in turn reveal the strength and weakness of radiomics.

Another limitation was the inconsistence in our training data set. This data set included different resolution and contrast-enhanced or non–contrast-enhanced CT scans. The window width/level used for the contouring were also slightly different. In the NSCLC radiomics collections lung and mediastinum windows are used, whereas in the ALK^+ set only the lung window was used. We believe these factors might introduce some bias and decrease model performance.

Conclusion

A preliminary study on the applicability of a general radiomic signature to ALK^+ patients with different treatment types was conducted. Our results indicate that it might be necessary in the future to develop a special radiomic signature for patients treated with targeted therapy.

Clinical Practice Points

- Previous research has identified the prognostic power of radiomics in NSCLC, but the conclusions developed from those findings are only applied to general NSCLC patients.
- Patients with ALK rearrangements usually exhibit unique clinical characteristics.
- Oncologists need effective tools to predict and improve their treatment outcome.
- Thus, in our preliminary study we assessed the performance of a radiomic signature developed in a general NSCLC for predicting the OS of ALK+ patients with different treatment types.
- We found its performance was impaired when the signature was applied to ALK+ patients who had received targeted therapy.
- That is to say, it could be necessary in the future to develop a special radiomic signature for patients treated with targeted therapy.
- In so doing, we hope that our research advances the development of a high-performance signature for patients with driver mutations.

Acknowledgments

Supported by Research Grant 14411965800 from the Science & Technology Commission of Shanghai Municipality.

Disclosure

The authors have stated that they have no conflicts of interest.

References

1. Ou SH, Bartlett CH, Mino-Kenudson M, Cui J, Iafrate AJ. Crizotinib for the treatment of ALK-rearranged non–small-cell lung cancer: a success story to usher in the second decade of molecular targeted therapy in oncology. *Onologist* 2012; 17:1351-75.
2. Gridelli C, Peters S, Sgambato A, Casaluce F, Adjei AA, Ciardiello F. ALK inhibitors in the treatment of advanced NSCLC. *Cancer Treat Rev* 2014; 40:300-6.
3. Soda M, Choi YL, Enomoto M, et al. Identification of the transforming EML4–ALK fusion gene in non–small-cell lung cancer. *Nature* 2007; 448:561.
4. Shaw AT, Yeap BY, Mino-Kenudson M, et al. Clinical features and outcome of patients with non–small-cell lung cancer who harbor EML4-ALK. *J Clin Oncol* 2009; 27:4247-53.
5. Shaw AT, Engelman JA. ALK in lung cancer: past, present, and future. *J Clin Oncol* 2013; 31:1105-11.
6. Yip SS, Aerts HJ. Applications and limitations of radiomics. *Phys Med Biol* 2016; 61:R150-66.
7. Limkin EJ, Sun R, Dercle L, et al. Promises and challenges for the implementation of computational medical imaging (radiomics) in oncology. *Ann Oncol* 2017; 28: 1191-206.
8. Gillies RJ, Kinahan PE, Hricak H. Radiomics: images are more than pictures, they are data. *Radiology* 2015; 278:563-77.
9. Coroller TP, Agrawal V, Narayan V, et al. Radiomic phenotype features predict pathological response in non–small-cell lung cancer. *Radiother Oncol* 2016; 119: 480-6.
10. Yu W, Tang C, Hobbs BP, et al. Development and validation of a predictive radiomics model for clinical outcomes in stage I non–small-cell lung cancer. *Int J Radiat Oncol Biol Phys* 2018; 102:1090-7.
11. Mattonen SA, Palma DA, Johnson C, et al. Detection of local cancer recurrence after stereotactic ablative radiation therapy for lung cancer: physician performance versus radiomic assessment. *Int J Radiat Oncol Biol Phys* 2016; 94:1121-8.
12. Ganeshan B, Panayiotou E, Burnand K, Dizdarevic S, Miles K. Tumour heterogeneity in non–small-cell lung carcinoma assessed by CT texture analysis: a potential marker of survival. *Eur Radiol* 2012; 22:796-802.
13. Huang Y, Liu Z, He L, et al. Radiomics signature: a potential biomarker for the prediction of disease-free survival in early-stage (I or II) non–small-cell lung cancer. *Radiology* 2016; 281:947-57.
14. Aerts HJ, Velazquez ER, Leijenaar RT, et al. Decoding tumour phenotype by noninvasive imaging using a quantitative radiomics approach [erratum in 2014; 5: 4644]. *Nat Commun* 2014; 5:4006.
15. Cunliffe A, Armato SG III, Castillo R, Pham N, Guerrero T, Al-Hallaq HA. Lung texture in serial thoracic computed tomography scans: correlation of radiomics-

based features with radiation therapy dose and radiation pneumonitis development. *Int J Radiat Oncol Biol Phys* 2015; 91:1048-56.
16. Cunliffe AR, Armato SG III, Straus C, Malik R, Al-Hallaq HA. Lung texture in serial thoracic CT scans: correlation with radiologist-defined severity of acute changes following radiation therapy. *Phys Med Biol* 2014; 59:5387-98.
17. Liu Y, Kim J, Qu F, et al. CT features associated with epidermal growth factor receptor mutation status in patients with lung adenocarcinoma. *Radiology* 2016; 280:271-80.
18. Thawani R, McLane M, Beig N, et al. Radiomics and radiogenomics in lung cancer: a review for the clinician. *Lung Cancer* 2018; 115:34-41.
19. Yang P, Kulig K, Boland JM, et al. Worse disease-free survival in never-smokers with ALK^+ lung adenocarcinoma. *J Thorac Oncol* 2012; 7:90-7.
20. Leijenaar RT, Carvalho S, Hoebers FJ, et al. External validation of a prognostic CT-based radiomic signature in oropharyngeal squamous cell carcinoma. *Acta Oncol* 2015; 54:1423-9.
21. Shaw AT, Kim DW, Nakagawa K, et al. Crizotinib versus chemotherapy in advanced ALK-positive lung cancer. *N Engl J Med* 2013; 368:2385-94.
22. Aerts HJWL, Rios Velazquez E, Leijenaar RTH, et al. Data From NSCLC-Radiomics. The Cancer Imaging Archive. Available at: http://doi.org/10.7937/K9/TCIA.2015.PF0M9REI. Accessed: October 1, 2016.
23. Clark K, Vendt B, Smith K, et al. The Cancer Imaging Archive (TCIA): maintaining and operating a public information repository. *J Digit Imaging* 2013; 26:1045-57.
24. Schemper M, Smith TL. A note on quantifying follow-up in studies of failure time. *Control Clin Trials* 1996; 17:343-6.
25. Galloway MM. Texture analysis using grey level run lengths. NASA STI/Recon Technical Report N. 1974 Jul;75. Available at: https://doi.org/10.1016/S0146-664X(75)80008-6.
26. Zhao B, James LP, Moskowitz CS, et al. Evaluating variability in tumor measurements from same-day repeat CT scans of patients with non−small-cell lung cancer. *Radiology* 2009; 252:263-72.
27. Zhao B, Schwartz LH, Kris MG. (2015). Data From RIDER_Lung CT. The Cancer Imaging Archive. Available at: http://doi.org/10.7937/K9/TCIA.2015.U1X8A5NR. Accessed: September 1, 2017.
28. Armato SG 3rd, Meyer CR, McNitt-Gray MF, et al. The Reference Image Database to Evaluate Response to therapy in lung cancer (RIDER) project: a resource for the development of change-analysis software. *Clin Pharmacol Ther.* 2008; 84:448-56.
29. Velazquez ER, Parmar C, Jermoumi M, et al. Volumetric CT-based segmentation of NSCLC using 3D-Slicer. *Sci Rep* 2013; 3:3529.
30. Kikinis R, Pieper S. 3D Slicer as a tool for interactive brain tumor segmentation. *Conf Proc IEEE Eng Med Biol Soc* 2011; 2011:6982-4.
31. Koo TK, Li MY. A guideline of selecting and reporting intraclass correlation coefficients for reliability research. *J Chiropr Med* 2016; 15:155-63.
32. Fried DV, Tucker SL, Zhou S, et al. Prognostic value and reproducibility of pretreatment CT texture features in stage III non−small-cell lung cancer. *Int J Radiat Oncol Biol Phys* 2014; 90:834-42.
33. Alexander BM, Othus M, Caglar HB, Allen AM. Tumor volume is a prognostic factor in non−small-cell lung cancer treated with chemoradiotherapy. *Int J Radiat Oncol Biol Phys* 2011; 79:1381-7.
34. Etiz D, Marks LB, Zhou SM, et al. Influence of tumor volume on survival in patients irradiated for non−small-cell lung cancer. *Int J Radiat Oncol Biol Phys* 2002; 53:835-46.
35. Fave X, Zhang L, Yang J, et al. Delta-radiomics features for the prediction of patient outcomes in non−small-cell lung cancer. *Sci Rep* 2017; 7:588.
36. Liu Y, Kim J, Balagurunathan Y, et al. Radiomic features are associated with EGFR mutation status in lung adenocarcinomas. *Clin Lung Cancer* 2016; 17:441-8.
37. Yamamoto S, Korn RL, Oklu R, et al. ALK molecular phenotype in non−small-cell lung cancer: CT radiogenomic characterization. *Radiology* 2014; 272:568-76.
38. Zhou M, Leung A, Echegaray S, et al. Non−small-cell lung cancer radiogenomics map identifies relationships between molecular and imaging phenotypes with prognostic implications. *Radiology* 2018; 286:307-15.
39. Andreassen CN, Schack LM, Laursen LV, Alsner J. Radiogenomics−current status, challenges and future directions. *Cancer Lett* 2016; 382:127-36.

Supplemental Appendix A

Radiomic Features Extraction

Texture features were extracted by using in-house codes on Matlab 2015b (MathWorks, Natick, MA). In total, 203 features were extracted. They are presented in Supplemental Table 2 in the online version. The following equations define some of these features.

1) Gray-Level Co-occurrence Matrix (GLCM) Features

Notation. $p(i,j) = i,j$th entry in a normalized gray-tone spatial-dependence matrix $= P(i,j)/R$

N_g = number of distinct gray levels in the quantized image

$p_x(i) = i$th entry in the marginal-probability matrix obtained by summing the rows of $p(i,j)$, $= \sum_{j=1}^{Ng} p(i,j)$

$$p_y(j) = \sum_{i=1}^{N_g} p(i,j)$$

$$p_{x+y}(k) = \sum_{j=1}^{Ng} \sum_{\substack{i=1 \\ i+j=k}}^{Ng} p(i,j), \quad \mathrm{k} = 2,3\ldots 2\,N_g$$

$$p_{x-y}(k) = \sum_{j=1}^{Ng} \sum_{\substack{i=1 \\ |i-j|=k}}^{Ng} p(i,j), \quad \mathrm{k} = 0,1,2,3\ldots N_g - 1$$

(1) Contrast

$$f_1 = \sum_{n=0}^{Ng-1} n^2 \left(\sum_{\substack{j=1 \\ |i-j|=k}}^{Ng} \sum_{i=1}^{Ng} p(i,j) \right)$$

(2) Correlation

$$f_2 = \frac{\sum_i \sum_j (ij)p(i,j) - \mu_x \mu_y}{\sigma_x \sigma_y}$$

Where $\mu_x, \mu_y, \sigma_x, \sigma_y$ are the means and standard deviations of $p_x(i)$ and $p_y(j)$

(3) Variance

$$f_3 = \sum_i \sum_j (i-\mu)^2 p(i,j)$$

(4) Entropy

$$f_4 = \sum_i \sum_j p(i,j)\log(p(i,j))$$

(5) Sum average

$$f_5 = \sum_{i=2}^{2Ng} i p_{x+y}(i)$$

(6) Sum variance

$$f_6 = \sum_{i=2}^{2Ng} (i - f_7)^2 p_{x+y}(i)$$

(7) Sum entropy

$$f_7 = -\sum_{i=2}^{2Ng} p_{x+y}(i)\log\left(p_{x+y}(i)\right)$$

(8) Difference variance

$$f_8 = \textit{variance of } p_{x-y}(k)$$

(9) Difference entropy

$$f_9 = -\sum_{i=0}^{Ng-1} p_{x-y}(i)\log\left(p_{x-y}(i)\right)$$

(10) and (11) Information measures of correlation

$$f_{10} = \frac{HXY - HXY1}{\max\{HX, HY\}}$$

$$f_{11} = (1 - \exp[-2.0(HXY2 - HXY)])^{1/2}$$

$$HXY = -\sum_i \sum_j p(i,j)\log(p(i,j))$$

Where HX and HY are entropies of p_x and p_y, and

$$HXY1 = -\sum_i \sum_j p(i,j)\log\left(p_X(i)p_y(j)\right)$$

$$HXY2 = -\sum_i \sum_j p_X(i)p_y(j)\log\left(p_X(i)p_y(j)\right)$$

(12) Maximal correlation coefficient

$$f_{12} = (\textit{second largest eigenvalue of } Q)^{1/2}$$

Where

$$Q(i,j) = \sum_k \frac{p(i,k)p(j,k)}{p_X(i)p_y(j)}$$

2) Gray-Level Run Length Matrix (GLRLM) Feature

Notation. $p_r(j) = \sum_{i=1}^{M} p(i,j)$

$$p_g(j) = \sum_{j=1}^{N} p(i,j)$$

(1) Short run emphasis (SRE)

$$\text{SRE} = \frac{1}{n_r}\sum_{i=1}^{M}\sum_{j=1}^{N}\frac{p(i,j)}{j^2} = \frac{1}{n_r}\sum_{j=1}^{N}\frac{p_r(j)}{j_2}$$

(2) Long run emphasis (LRE)

$$\text{LRE} = \frac{1}{n_r}\sum_{i=1}^{M}\sum_{j=1}^{N}p(i,j)j^2 = \frac{1}{n_r}\sum_{j=1}^{N}p_r(j)j^2$$

(3) Gray-level nonuniformity (GLN)

$$\text{GLN} = \frac{1}{n_r}\sum_{i=1}^{M}\left(\sum_{j=1}^{N}p(i,j)\right)^2 = \frac{1}{n_r}\sum_{i=1}^{M}p_g(i)^2$$

(4) Run length nonuniformity (RLN)

$$\text{RLN} = \frac{1}{n_r}\sum_{j=1}^{N}\left(\sum_{i=1}^{M}p(i,j)\right)^2 = \frac{1}{n_r}\sum_{j=1}^{N}p_r(i)^2$$

(5) Run percentage (RP)

$$\text{RP} = \frac{n_r}{n_p}$$

In the GLRLM formulas 1 to 5, n_r is the total number of runs and n_p is the number of pixels in the image.

(6) Low gray-level run emphasis (LGRE)

$$\text{LGRE} = \frac{1}{n_r}\sum_{i=1}^{M}\sum_{j=1}^{N}\frac{p(i,j)}{i^2} = \frac{1}{n_r}\sum_{i=1}^{M}\frac{p_g(i)}{i_2}$$

(7) High gray-level run emphasis (HGRE)

$$\text{HGRE} = \frac{1}{n_r}\sum_{i=1}^{M}\sum_{j=1}^{N}p(i,j)i^2 = \frac{1}{n_r}\sum_{j=1}^{N}p_g(i)i^2$$

(8) Short run low gray-level emphasis (SRLGE)

$$\text{SRLGE} = \frac{1}{n_r}\sum_{i=1}^{M}\sum_{j=1}^{N}\frac{p(i,j)}{i^2j^2}$$

(9) Short run high gray-level emphasis (SRHGE)

$$\text{SRHGE} = \frac{1}{n_r}\sum_{i=1}^{M}\sum_{j=1}^{N}\frac{p(i,j)i^2}{j^2}$$

(10) Long run low gray-level emphasis (LRLGE)

$$\text{LRLGE} = \frac{1}{n_r}\sum_{i=1}^{M}\sum_{j=1}^{N}\frac{p(i,j)j^2}{i^2}$$

(11) Long run high gray-level emphasis (LRHGE)

$$\text{LRHGE} = \frac{1}{n_r}\sum_{i=1}^{M}\sum_{j=1}^{N}p(i,j)i^2j^2$$

Supplemental Figure 1 The Intraclass Correlation Coefficient (ICC) Distribution in Each Feature Group. We Counted the Number of Features Within Different ICC Intervals (Binwidth: 0.025). Except for Gray-Level Run Length Matrix , Wavelet Transformation Could Improve Feature Stability. The Dashed Line Represents the ICC Value of 0.9

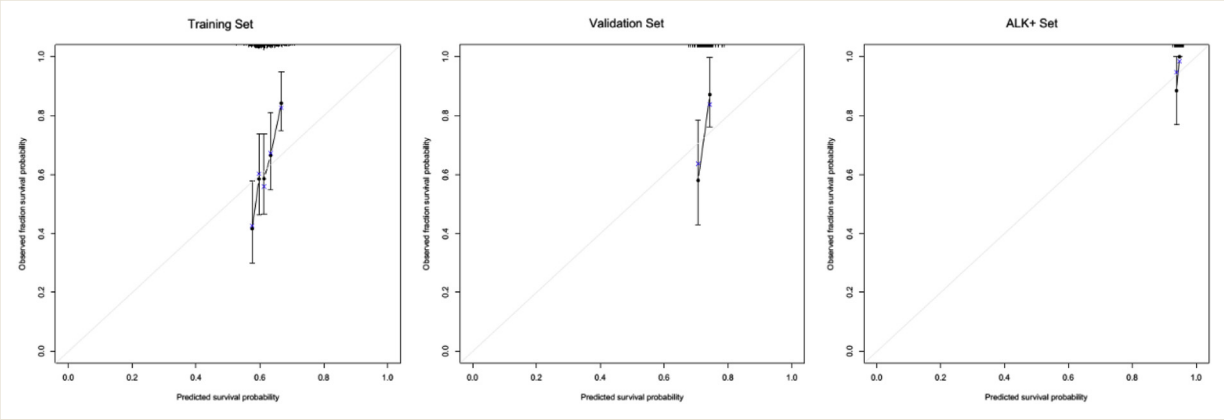

Supplemental Figure 2 Calibration Curve for 1-Year Survival in the Training, Validation, and ALK^{+} Set

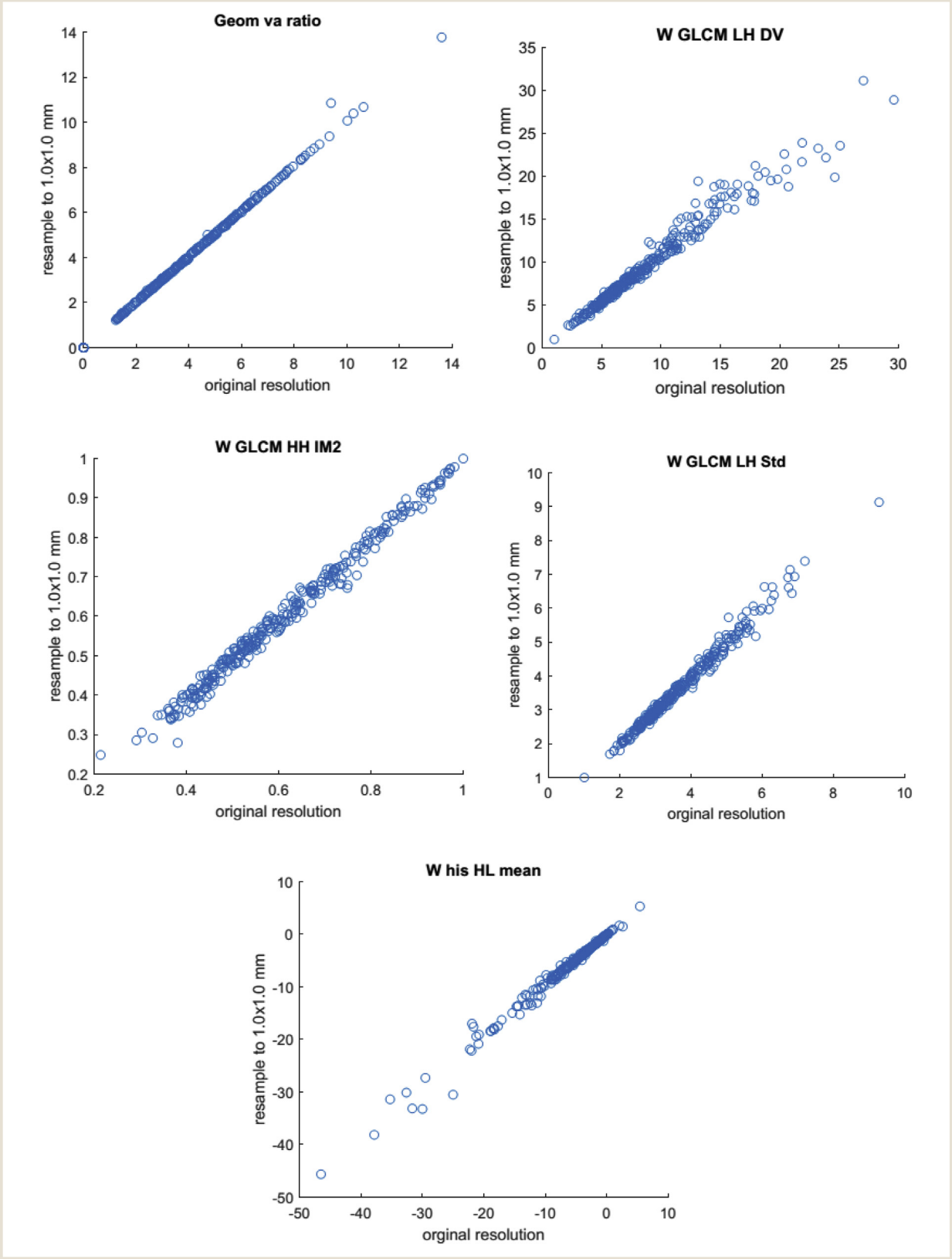

Abbreviation: ALK = anaplastic lymphoma kinase.

Supplemental Table 1 Four Types of Radiomic Features

Types	Feature Type 1. Geometry Features	Feature Type 2. Histogram Features	Feature Type 3. Texture Features		Feature Type 4. Wavelet Features
			Gray-Level Co-Occurrence Matrix-Based Features	Gray-Level Run-Length Matrix-Based Features	
Number	3	9	20	11	160
Definition	Volume	Mean	Contrast	Short run emphasis	Wavelet histogram feature
	Area	Median	Correlation	Long run emphasis	Wavelet GLCM
	VolumeArea_Ratio	Variance	Energy	Gray-level nonuniformity	Wavelet GLRM
		Skewness	Homogeneity	Run length nonuniformity	
		Kurtosis	Mean	Run percentage	
		Minimum	Variance	Low gray-level run emphasis	
		Maximum	Std	High gray-level run emphasis	
		Std	Dissimilarity	Short run low gray-level emphasis	
		Range	Entropy	Short run high gray-level emphasis	
			Sum_average	Long run low gray-level emphasis	
			Difference_average	Long run high gray-level emphasis	
			Sum_variance		
			Difference_variance		
			Sum_Entropy		
			Difference_Entropy		
			Information_Measures_I		
			Information_Measures_II		
			Maximal_Correlation_Coefficient		
			Homogeneity_Original		
			Correlation_Original		

A total of 203 radiomic features were extracted in this study.

Supplemental Table 2 Test-Retest Results

ICC	Geometry	Histogram	GLCM	GLRLM	W_GLCM	W_GLRLM	W_Histogram
≥0.9	3	3	9	9	67	17	24
0.75-0.9	0	5	10	1	3	11	8
0.5-0.75	0	1	0	1	10	13	4
<0.5	0	0	1	0	0	3	0

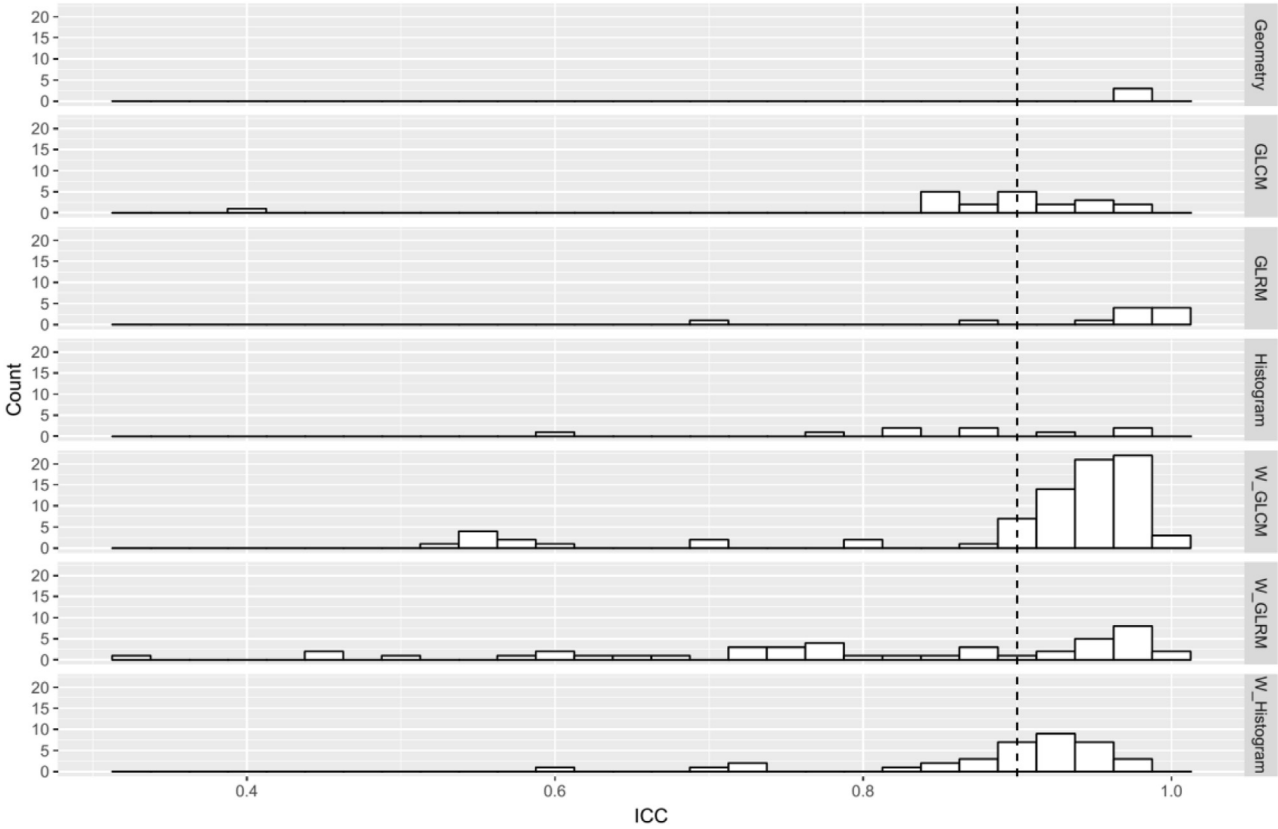

Abbreviations: GLCM = Gray-Level Co-occurrence Matrix based features; GLRLM= Gray-Level Run Length Matrix based features; W_GLCM = Wavelet transformed Gray-Level Co-occurrence Matrix based features; W_GLRM = Wavelet transformed Gray-Level Run Length Matrix based features; W_histogram= Wavelet transformed histogram based features.

Supplemental Table 3	The Selected Features' Abbreviations
Geom_va_ratio	Geometry feature_volume to area ratio
W_GLCM_Std	Wavelet transformed GLCM_Standard deviation
W_GLCM_DV	Wavelet transformed GLCM_Difference Variance
W_GLCM_IM2	Wavelet transformed GLCM_Information Measures II
W_his_mean	Wavelet transformed Histogram_mean